ISSN 0023-1584, Kinetics and Catalysis, 2012, Vol. 53, No. 5, pp. 570–576. © Pleiades Publishing, Ltd., 2012.
Original Russian Text © R.A. Zotov, A.A. Glazyrin, V.V. Danilevich, I.V. Kharina, D.A. Zyuzin, A.M. Volodin, L.A. Isupova, 2012, published in Kinetika i Kataliz, 2012, Vol. 53, No. 5, pp. 599–606.

Influence of the Temperature of Calcination of Bayerite-Containing Aluminum Hydroxide Pellets on the Water Vapor Adsorption Capacity and Acid–Base Properties of Alumina

R. A. Zotov, A. A. Glazyrin, V. V. Danilevich, I. V. Kharina, D. A. Zyuzin, A. M. Volodin, and L. A. Isupova

Boreskov Institute of Catalysis, Siberian Branch, Russian Academy of Sciences, Novosibirsk, 630090 Russia
e-mail: isupova@catalysis.ru

Received March 17, 2011

Abstract—The paper considers the influence of the temperature of calcination (350–550°C) of alumina-based water adsorbents prepared from bayerite-containing aluminum hydroxide on the static water sorption capacity at high and low relative air humidities and on the acid–base properties of the surface. The acid–base properties of aluminas have been determined by means of IR spectroscopy of adsorbed CO probe molecule (Lewis sites) and by the spin probe method, which was used to determine the concentrations of electron acceptor and electron donor sites. It has been demonstrated that, at a high relative air humidity (60%), there is no correlation between the static capacity of the drier and its acid–base properties, while at low relative humidities (1–1.5%), an increase in the concentration of electron donor sites and a decrease in the concentration of electron donor and Lewis acid sites enhance the water sorption capacity of alumina.

DOI: 10.1134/S0023158412050187

The moisture that is present in industrial hydrocarbon streams can have significant influence on the efficiency of many processes. For example, high humidity significantly reduces the activity of hydrocarbon alkylation and oligomerization catalysts. The optimal humidity of circulating gases is necessary for maintaining the catalyst in the active state in catalytic reforming [1]. Drying of hydrocarbon gases is necessary for the transportation of natural gas in order to prevent the formation of hydrocarbon gas hydrates and water slugs [2].

Aluminum oxides have been used for a long time as adsorbents for drying of different industrial gases (air and natural gas). For the first time, alumina was used in water adsorption by ALCOA company in 1932. The wide application of aluminas as water sorbents is due to both their high efficiency in the drying of gases with a relative humidity of 1 to 100% [3] and the fact that alumina shaped as pellets or extrudates has a high abrasion resistance and breaking strength and withstands many regeneration cycles without changing its water sorption capacity [4]. Aluminas can be used as the matrix for deposition of various hygroscopic compounds increasing their water sorption capacity and allow maintaining a constant (optimal) humidity of the medium owing to the reversibility of the hydration–dehydration process [5–8].

The rapid development of petrochemical technologies, as well as the competition in economy, constantly raise the requirements for alumina driers, including an increase in their water sorption capacity (degree of drying) at a given relative humidity. At present, the well-known basic principles of design of gas drying apparatuses include calculation of the diameter and length of the reactor, gas flow rate, heat removal, and regeneration conditions for the required level of gas drying [9–11]. The principles of sorption of carious molecules, including water, as a result of their concentration on the surface of a solid are also known. It is believed that the amount of adsorbed compound is directly related to the surface area accessible to the sorbate. The porous structure also plays an important role in water sorption [4]. So far, the nature of the forces that hold particular molecules on the surface has not been completely understood and a number of theories have been proposed for explanation of this phenomenon [4]. The best known theory is the one proposed by Langmuir, which assumes that the interaction of water molecules with the surface is mainly physical in nature (coordination, van der Waals, dipole–dipole and quadrupole interactions) [2, 4, 12, 13]. For example, it was suggested that water sorption occurs through the formation of adducts of the $H^+(H_2O)_n$ type on high-silica zeolites as a result of the interaction of water molecules with Brønsted acid sites [14]. At the same time, individual aluminas without strong Brønsted acidic sites [15] also adsorb water well and, consequently, other sites can also participate in water sorption. IR spectroscopy method has shown that there are strong Lewis acid sites on the surface of aluminum oxide [15]. The spin probe method has revealed that the surface of aluminum oxides has elec-

tron acceptor and electron donor sites capable of reducing (oxidizing) adsorbed molecules due to the transfer of one electron (Single Electron Transfer (SET) mechanism) [16–19]. It is reasonable to assume that the change of the concentration of the mentioned sites can influence the physicochemical properties of the surface and, therefore, the sorption rate and sorption capacity of alumina.

An important stage of alumina preparation is calcination which can dramatically influence the ratio of Lewis acid sites (LAS's) and Brønsted acid sites (BAS's) (electron donors and acceptors, respectively) on the surface of the oxide and, consequently, its acid–base properties and water vapor sorption capacity.

The present study considers the influence of the temperature of the preparation of aluminas on their acid–base properties and static (equilibrium) water vapor sorption capacity in the humidity range from 1 to 60%. The original compound was bayerite-containing hydroxide obtained by the thermochemical activation (TCA) technology [20]. The specific feature of bayerite-containing hydroxide is the formation of low-temperature alumina (first of all, η-modification) at a calcination temperature of >300°C, which enable obtaining samples with a large specific surface area, with a large number of micropores, and, accordingly, with a higher static capacity than that of the water sorbents based on γ-Al_2O_3. In addition, the acid–base properties of such water sorbents will obviously differ from the properties of γ-Al_2O_3 prepared from pseudoboehmite.

The aim of the present study was to investigate the influence of the temperature of calcination of the pellets of the alumina-based adsorbent prepared from bayerite-containing hydroxide (product of the thermochemical activation of hydrargillite) on the static water vapor sorption capacity at high (60%) and low (1–1.5%) relative humidities and to study of the role of the acid–base properties of the resulting samples in water sorption.

EXPERIMENTAL

Preparation of Alumina Adsorbents

The original material was thermally activated aluminum hydroxide (OAO Achinsk Alumina Refinery, Specifications TU 1711-001-05785164-2002). The powder was hydrated in a ball mill at room temperature in a solution of NH_3 at pH 11–12 for 24 h at a component ratio of 1 : 1.

The dried powder was plasticized with a solution of nitric acid (acidic modulus of 0.1 mol acid/mol Al_2O_3). The resultant paste was extruded in a ram extruder through a die with a hole diameter of 4 mm. The pellets were calcined in a tubular furnace in flowing dry air for 4 h. The temperature of calcination of the pellets was varied in the 350–550°C range in 50-deg steps. The chosen temperature interval (350–550°C) was especially interesting for investigation of the properties of alumina as a water sorbent.

For comparison, we used 100% γ-Al_2O_3 (T_{calcin} = 550°C), which was obtained by conventional reprecipitation [21].

Investigation of the Physicochemical and Water Sorption Properties of Alumina Adsorbents

X-ray diffraction (**XRD**) analysis of the samples was carried out using an HZS-4 diffractometer (Germany) with monochromated CuK_α radiation (λ_{av} = 1.54184 Å). Diffraction patterns were recorded in the 2θ range from 10° to 75°. The phase composition of aluminum hydroxide and alumina, unit cell parameters, and crystallite sizes were determined from the diffraction patterns. In quantitative phase analysis, we used plots of diffraction peak intensity ratios versus the concentration of reference phases [22].

Thermal analysis was carried out using an STA 449 C Jupiter apparatus (NETZSCH, Germany) in the temperature range from 20 to 1000°C.

The thermoanalytical curves—T, DTA, TG, and DTG—were recorded under the following conditions: heating rate of 10 deg/min, air flow rate of 30 mL/min, sample weight of 100 mg, corundum crucibles, calcined alumina was the reference sample.

The textural properties of alumina were investigated by means of low-temperature nitrogen desorption at 77 K using an Asao 2400 analyzer (Micromeritics, United States). The specific surface area was calculated using the BET equation. The micropore volume and the mesopore surface area remaining after micropore filling were determined by a comparative method [23, 24].

Acid–base sites on the surface were quantified spectroscopically using the adsorption of CO probe molecule [25, 26]. IR spectra were recorded on a Shimadzu 8300 Fourier spectrometer (Japan) with 4 cm^{-1} resolution and 100 coadditions per data point. The spectra were processes using the ORIGIN software package. The error in the concentration measurements was ±15%. Before CO adsorption, the sample was heated in a vacuum at 300°C for 1.5 h. The adsorption of CO was performed at the liquid nitrogen temperature and a pressure of 0.1–10 Torr. The concentration of Lewis acid sites was derived from the absorption bands at 2183–2186 cm^{-1}, which appeared as a result of the adsorption of CO molecules on LAS's at a CO pressure of 0.1 Torr. The concentration of OH groups was determined from the absorption band at 2152 cm^{-1}, which appeared as a result of CO adsorption on BAS's at a CO pressure of 10 Torr.

The concentration of electron donor and electron acceptor sites was determined using the spin probe method [16–19]. Before the experiments, the samples were dehydrated at 300°C in air. The probes for electron donor sites were the radicals generated by the adsorption of the acceptor molecules of trinitroben-

Table 1. Phase composition and structural characteristics of the original aluminum hydroxide and alumina samples

Sample	a*, Å	Phase composition, % (D, Å)					
		gibbsite	bayerite	boehmite	pseudoboemite	$(\gamma + \eta)$-Al_2O_3	X-ray-amorphous phase + χ-Al_2O_3
SW-5	7.89	13	51	1 (155)	–	–	35
Al_2O_3-350	7.92	–	–	10 (240)	~2 (35)	30 (45)	58
Al_2O_3-450	"	–	–	–	–	35 (45)	65
Al_2O_3-550	"	–	–	–	–	45 (50)	55
γ-Al_2O_3	"	–	–	–	–	100 (40)	–

* Unit cell parameter averaged over all phases.

zene (0.02 M solution in toluene). For the diagnostics of electron acceptor sites, we used the radical that appeared as a result of the adsorption of the donor molecules of anthracene (0.04 M solution in toluene). In all cases, the ultimate concentration of radicals was determined after keeping the samples with adsorbed probe molecules at 80°C for 12 h using an ESR-221 EPR spectrometer (Germany) which operating in the X-band frequency range (9.3 GHz). The power of the microwave radiation in the resonator was up to 200 mW, and the attenuation of the radiated power was below 60 dB. The sensitivity of the spectrometer at a constant time of $\tau = 1$ s was 3×10^{10} spin/10^{-4} T. The error in the concentration measurements was ±10%.

Determination of the Equilibrium Adsorption Capacity

The static (equilibrium) water vapor capacity of the driers was determined in a flow apparatus with a ~10-cm^3 quartz reactor at atmospheric pressure and room temperature. The apparatus was placed into a glass heating chamber in which a constant temperature (20–21°C) was maintained. A bubbler filled with water (Drexel bottle), a tube with a zeolite, and a cylinder with compressed air were also placed in the heating chamber. This allowed reliable results to be obtained under identical conditions. Before being loaded into the reactor, the water adsorbent was calcined at 300°C for 4 h. The adsorbent weight was 0.5 g (pellet size of 0.5–1 mm), the height of the adsorbent bed was 1 cm, and the total air feed rate was 20 L/h. The relative humidity of the supplied air was varied from 1 to 60% (normalized to 20°C) using gas flow controllers. For this purpose, two air streams were created. One of them was preliminary dried by passing it through a tube filled with zeolite NaA, and the other was saturated with water to a relative humidity of ~90% in a bubbler (Drexel bottle). The streams were combined in a mixer. After that, the combined air stream with a preset humidity was fed into the reactor. The air humidity at the inlet and outlet of the reactor was monitored using an IVA-6B thermohygrometer (Mikrofor, Russia).

It was assumed that the equilibrium was established when the humidity at the outlet of the reactor was the same as its value at the inlet. Thereafter, the adsorbent was withdrawn from the reactor and was weighed. All measurements were carried out at room temperature (20–21°C) at a low relative air humidity in the laboratory. Under these conditions, we studied the rate of water adsorption after the sample was exposed to the atmosphere. For this purpose, preliminarily dried samples were weighed at 5-min intervals over 1 h. After 1 h, the weight gain was 1–1.5 wt %. Therefore, the short-term exposure of the samples to the atmospheric conditions hardly influenced the value of the experimental error.

The water vapor capacity was calculated using the following equation:

$$\text{Capacity, } \% = 100(m_a - m_{0)}/m_0,$$

where m_0 and m_a is the weight of the adsorbent before and after water adsorption, respectively.

The error in the measurements of static capacity was ±10%.

The results of the measurements were compared with the data of vacuum adsorption method at relative air humidities of 10% (supersaturated solution of orthophosphoric acid) and 60% (supersaturated solution of NaBr). The results of these measurements coincided.

RESULTS AND DISCUSSION

Phase Composition and Textural Characteristics of Alumina

The phase compositions of the original bayerite-containing hydroxide (SW-5), the adsorbents prepared in this study, and the reference sample are presented in Table 1. This table shows that the original hydroxide contained over 50% crystalline bayerite, 13% gibbsite, and 35% amorphous phase, which can apparently be classified as X-ray-amorphous hydroxide and hydrated χ-phase. The concentration of boehmite in the sample did not exceed 1%, and no pseudoboehmite was found.

Table 2. Influence of the temperature of the synthesis of alumina samples on their textural characteristics

Sample	S_{BET}, m^2/g	$V_{pore\ total}$, cm^3/g	V_{pore} (1.7–300 nm), cm^3/g	V_{pore} (<1.7 nm), cm^3/g	$D_{pore\ mean}$, Å
Al_2O_3-350	327	0.24	0.10	0.11	22.0
Al_2O_3-400	390	0.27	0.12	0.16	28.0
Al_2O_3-450	343	0.26	0.12	0.13	30.0
Al_2O_3-500	340	0.27	0.13	0.12	31.8
Al_2O_3-550	328	0.28	0.15	0.10	33.8
γ-Al_2O_3	294	0.67	0.57	0	92.0

According to the data of thermal analysis, the calcination of the original hydroxide from 20 to 1000°C gives rise to three endothermic peaks. The first one (at 80–200°C) can be assigned to the loss of adsorbed and chemisorbed water; the second one (at 280–340°C), to the conversion of gibbsite and bayerite into χ-Al_2O_3 and η-Al_2O_3, respectively; the third one (at 500–560°C), to the conversion of boehmite (pseudoboehmite) into γ-Al_2O_3. The thermoanalytical data indicate that the initial hydroxide contains 55% trihydroxide phases (bayerite + gibbsite) and 11% boehmite (pseudoboehmite). The difference between the TA and XRD data indicate that either the original hydroxide contains an X-ray amorphous phase of pseudoboehmite or boehmite (pseudoboehmite) forms inside the gibbsite and bayerite particles during thermal treatment as a result of the creation of hydrothermal conditions. We were unable to distinguish the thermoanalytical peak due to the conversion of aluminum trihydroxide into boehmite (180°C) against the background of the broad endotherm (80–200°C) due to the loss of both physically adsorbed and chemisorbed water.

X-ray diffraction analysis of the alumina samples (Table 1) obtained by the calcination of bayerite-containing hydroxide (SW-5) in flowing dry air at 350, 450, and 550°C showed that the Al_2O_3-350 sample contains over 50% X-ray amorous phase (hydroxide/oxide + χ-Al_2O_3), approximately 30% (γ + η)-Al_2O_3, 10% boehmite, and a small amount of pseudoboehmite. Since the conversion of the X-ray amorphous hydroxide/oxide into the well-crystallized boehmite phase as a result of calcination is unlikely, it can be concluded that boehmite results from the decomposition of the trihydroxides (gibbsite and bayerite). The sample obtained by the calcination of SW-5 at 450°C (Al_2O_3-450) contains about 35% (γ + η)-Al_2O_3 and 65% amorphous phase (hydroxide/oxide + χ-Al_2O_3). The XRD data did not indicate the presence of boehmite in Al_2O_3-450 sample. Since the temperature of 450°C was not sufficient for the formation of crystalline γ-Al_2O_3, we suppose that, at this stage, pseudoboehmite can turn into amorphous alumina. This assumption is confirmed by the increase in the proportion of the (amorphous hydroxide/oxide + χ-Al_2O_3) phases (Table 1) and by the absence of the pseudoboehmite decomposition endotherm in the 500–550°C range for the Al_2O_3-450 sample. Raising the temperature to 500–550°C results in the crystallization of part of the X-ray amorphous phase of alumina and in the formation of γ-Al_2O_3. The Al_2O_3-550 sample contains about 45% crystalline phases (γ + η)-Al_2O_3 and 55% χ-Al_2O_3.

Therefore, the prepared samples are heterogeneous and consist of amorphous and crystalline phases, and the difference between their phase compositions does not exceed 10% as the calcination temperature is increased. The low-temperature samples contain pseudoboehmite.

Table 2 lists the textural characteristics of the tested samples of alumina. All of the samples have a high specific surface area (over 320 m^2/g). As the calcination temperature is raised, the specific surface area (as well as the micropore volume and surface area) passes through an extremum at 400°C. This behavior can possibly be due to the complete decomposition of hydroxides and the formation of alumina followed by the sintering of the latter. The average specific surface area of the sample calcined above 400°C is 340 m^2/g, higher than that of, e.g., γ-Al_2O_3; even after calcination at 550°C, the oxides have micropores, unlike the reference sample. The mean pore radius of the prepared samples is 3 times smaller than that of the reference sample. The mean pore volume remains practically invariable as the calcination temperature is raised. The micropore volume is largest for the sample calcined at 400°C. Therefore, the increase in the calcination temperature mainly affects the micropore volume and surface area. The synthesized samples are significantly different from the reference sample in terms of both phase composition and texture.

Acid–Base Properties of Alumina

It was established that, as the calcination temperature is elevated, the concentration of electron acceptor sites (including weak ones) per gram of water adsorbent initially decreases (350–450°C), then increase by a factor of 1.5 (500°C), and then again decreases as the calcination temperature grows to 550°C (Table 3). The same trend was observed also for the concentration of electron acceptor sites per unit area of the surface

Table 3. Influence of the temperature of the synthesis of alumina samples on their static capacity and acid–base properties

Sample	Static capacity, %		$N_{acc}^* \times 10^{-16}$	$N_{don}^* \times 10^{-17}$	$N_{acc}^* \times 10^{-14}$	$N_{don}^* \times 10^{-15}$	LAS (2183–2186 cm^{-1})		OH groups (2155 cm^{-1})	
	relative humidity, %		g^{-1}		m^{-2}		μmol/m^2	μmol/g	μmol/m^2	μmol/g
	1–1.5	60								
Al_2O_3-350	3.6	17.9	9.5	0.99	2.91	0.30	284	0.87	1.22	400
Al_2O_3-400	3.5	21.6	8.3	5.78	2.13	1.48	520	1.33	1.01	395
Al_2O_3-450	2.5	20.5	7.6	8.40	2.22	2.45	607	1.77	1.24	425
Al_2O_3-500	2.1	19.5	11.1	11.62	3.38	3.54	511	1.56	1.07	365
Al_2O_3-550	1.9	19.0	9.9	10.56	2.91	3.11	559	1.64	1.10	360

* Number of acceptor and donor sites, respectively.

(1 m^2), indicating a change in the chemical properties of the surface. The concentration of electron donor sites increases steadily as the calcination temperature is increased to to 500°C and remains practically unchanged at higher temperatures.

The concentration of Lewis acid sites determined by IR spectroscopy increases with an increasing calcination temperature (350–450°C), then falls (500°C), and then again increases as the temperature is increased to 500–550°C (Table 3). The increase in the LAS concentrations with an increase in calcination temperature to 450°C can occur as a result of both the increase in the alumina concentration due to the decomposition of pseudoboehmite and the dehydroxylation of the alumina surface, i.e., the decrease in the BAS concentration. The concentrations of LAS's (per gram of adsorbent) and electron acceptor sites (per gram of adsorbent) vary with temperature in opposite ways. Therefore, it can be assumed that the electron acceptor sites are related with strong BAS's, whose concentration should decrease with an increase in the calcination temperature. We proposed this hypothesis when we developed a procedure for the determination of the concentration of electron acceptor sites and investigated the influence of the concentration of these sites on catalytic activity in the dehydration of alcohols into olefins [26]. The observed reduction of the LAS concentration and the increase in the concentration of electron acceptor sites (Table 3) for the samples calcined at 450–500°C can be due to the stronger bonding of hydroxyl groups with the surface aluminum cations in these samples as a result of, for example, the increase in the proportion of crystalline phases ($\gamma + \eta$)-Al_2O_3.

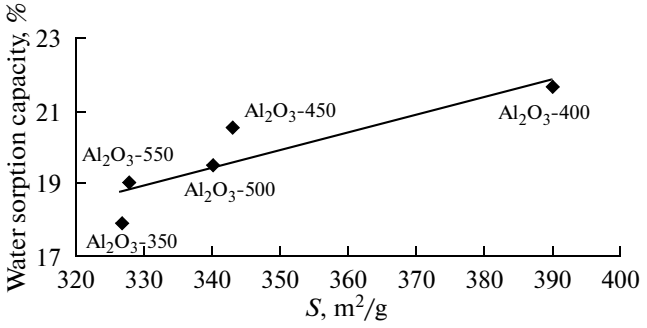

Fig. 1. Influence of the specific surface area of alumina on its static water sorption capacity at a relative air humidity of 60% at 20°C.

According to IR spectroscopic data, the alumina samples contain mainly weak BAS's (absorption band at 2152 cm^{-1}, $P(CO) = 10$ Torr). The total concentration of these sites per unit area of the surface remains practically invariable as the calcination temperature is increased (Table 3).

Static Sorption Capacity and Acid–Base Properties of Alumina

The static capacity of aluminum oxides was determined at high (60%) and low (1–1.5%) relative air humidities.

At an air humidity of 60%, we obtained a nearly linear correlation between the static capacity of the samples and their specific surface area (Fig. 1). The deviation from linearity could be due to the variation of the pore size distribution, since the total pore volume of the samples was nearly the same. The concentrations of electron acceptor and electron donor sites (determined by the spin probe method) and LAS's are not correlated with the static capacity measured at 60% relative air humidity. This result implies that, at high air humidity under conditions of volume filling of micro- and mesopores, the difference between the acid–base properties of the sample surfaces does not manifest itself and the static capacity of the adsorbent is determined by the total pore volume and pore size distribution.

We assumed that the influence of the acid–base properties is more pronounced at low relative humidity in the region of filling of micropores (<1.7 nm). A distinctive feature of micropores is that their opposite

walls are extremely close together walls, leading to the overlap of the electric fields of the surfaces of the neighboring walls. Therefore, it is impossible to apply the so-called theory of volume filling of micropores [4]. Varying the concentration of electron acceptor, electron donor, and Lewis acid sites, one can modify the physicochemical properties of the surface in a certain range and thereby, influence the possibility of volume filling of the micropores with water molecules.

In order to estimate the effect of relative humidity on the static capacity of a water adsorbent and choose the conditions for filling its micropores only, we investigated the static water sorption capacity of the adsorbents at relative air humidities from 60 to 1%. The tests were carried out for the Al_2O_3-400 sample, which was obtained by calcination at 400°C. The reference sample did not contain micropores. The plots presented in Figs. 2 and 3 demonstrate that the static capacity grows with increasing relative air humidity. This indicates that, as the partial pressure of water vapor is increased, capillary condensation proceeds into pores of larger size. The shape of the curve also allows indirect estimation of the pore size distribution for the tested adsorbents. Since the reference sample, which does not contain micropores (Table 2), adsorbs water at relative air humidities above 1–2% (Figs. 2, 3), it may be assumed that, at lower humidities, water sorption occurs only in micropores with a radius of <1.7 nm. Thus, we have determined the relative air humidity at which the micropores are mainly filled; it appeared to be 1–1.5%.

At a low humidity (1–1.5%), the static capacity decreases with an increasing adsorbent pellet calcination temperature. This is accompanied by an increase in the concentration of electron donor sites (Table 3). The total micropore volume initially (350–400°C) increases and then (400–550°C) decreases (Table 2). An inverse correlation with a confidence factor of 0.85 was observed between the static capacity and the concentration of electron donor sites (Fig. 4). The deviation from linearity can be due to the tested samples differing in micropore volume.

There is seemingly no general correlation between the concentration of electron acceptor sites and LAS's and the static capacity. However, if the samples calcined at 350–550°C are divided into two groups—those calcined at 350–450°C and those calcined at 500–550°C—it will be clear that an increase in the concentration of electron acceptor sites (supposedly related with Brønsted acidity [27]) and a decrease in the concentration of LAS's leads to an increase in the static water sorption capacity at low humidity (1–1.5%) (Table 2). The absence of a general linear correlation can be a consequence of the additional influence of the pore size distribution and of the absence of pseudoboehmite in the samples calcined above 450°C.

Therefore, we have investigated the influence of calcination temperature in the 350–550°C range on the static (equilibrium) capacity at low (1–1.5%) and high (60%) relative humidities and on the acid–base properties, phase composition, and texture of the alumina-based adsorbents obtained by calcination of bayerite-containing hydroxide.

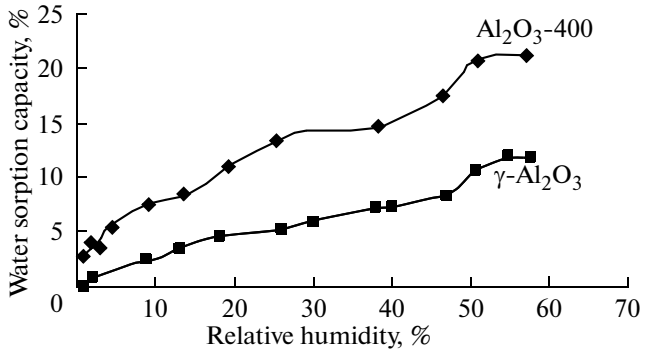

Fig. 2. Influence of relative air humidity in the 1–60% range on the static capacity of Al_2O_3-400 and the reference sample γ-Al_2O_3 at 20°C.

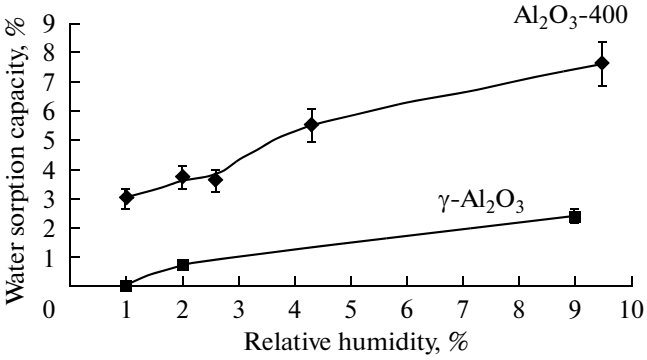

Fig. 3. Influence of relative air humidity in the 1–10% range on the static capacity of Al_2O_3-400 and the reference sample γ-Al_2O_3 at 20°C.

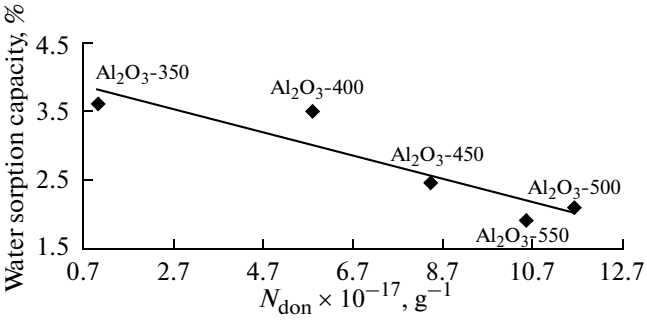

Fig. 4. Influence of the concentration of electron donor sites on the static capacity of alumina samples at a relative air humidity of 1–1.5% at 20°C.

We have shown that the relative activity of the adsorbents measured at low (1–1.5%) and high (60%) humidities can be different. Since the humidity of the entering gases in many industrial drying units is below 3%, we recommend a procedure for determination of

water sorption capacity of adsorbents at low humidity (1–3%), which, in our opinion, better simulates industrial drying stages. (Nowadays the procedure used in plants for determination of the activity of adsorbents is based on measuring the static capacity at relative air humidities of 10 and 60%.)

We have established that acid–base properties of alumina have an effect on the static water sorption capacity at low relative humidity (1–1.5%). An increase in the concentration of electron acceptor sites (apparently related with Brønsted acidity) and a decrease in the concentration of electron donor and Lewis acid sites lead to an increase in the static water sorption capacity of the samples. Therefore, the presence of hydroxylated surface is favorable for water adsorption at low humidity. The static water sorption capacity also depends on the phase composition and micropore size distribution. It seems impossible to estimate the effect of each of these factors from the experimental data of this study, so this will be a subject of forthcoming studies.

At high relative humidity (60%), the static water sorption capacity depends mainly on the volume of the pores where capillary condensation takes place. The concentration and strength of the electron acceptor (acidic) and electron donor (basic) surface sites should be sufficient for the adsorption of the first layer of water molecules (surface wetting); i.e., at high humidity the acid and basic sites initiate the process, while the sorption capacity is determined by the pore volume of the adsorbent.

REFERENCES

1. Buluchevskii, E.A., Lavrenov, A.V., and Duplyakin, V.K., *Ross. Khim. Zh.*, 2007, vol. 51, no. 4, p. 85.
2. Kohl, A.L. and Nielsen, R.B., *Gas Purification*, Houston: Gulf, 1997.
3. Fleming, H.L., *Stud. Surf. Sci. Catal.*, 1999, vol. 120, no. 1, p. 561.
4. Ruthven, D.M., Farooq, S., and Knaebel, K., *Pressure Swing Adsorption*, New York: VCH, 1994.
5. Aristov, Yu.I., Restuccia, G., Cacciola, G., and Parmon, V.N., *Appl. Therm. Eng.*, 2002, vol. 22, p. 191.
6. Gordeeva, L.G., Resticcia, G., Cacciola, G., and Aristov, Yu.I., *React. Kinet. Cat. Lett.*, 1998, vol. 63, no. 1, p. 81.
7. Aristov, Yu.I., Tokarev, M.M., DiMarko, G., Cacciola, G., Restuccia, D., and Parmon, V.N., *Russ. J. Phys. Chem.*, 1997, vol. 71, no. 2, p. 197.
8. Gordeeva, L.G., Restuccia, D., Tokarev, M.M., Cacciola, G., and Aristov, Yu.I., *Russ. J. Phys. Chem.*, 2000, vol. 74, no. 12, p. 2016.
9. White, D.H. and Barkley, P.G., *Chem. Eng. Prog.*, 1989, vol. 85, no. 1, p. 25.
10. Cruz, P., Santos, J.C., Magalhaes, F.D., and Mendes, A., *Chem. Eng. Sci.*, 2003, vol. 58, p. 3143.
11. Nilchan, S. and Pantelides, C.C., *Adsorption*, 1998, vol. 4, p. 113.
12. Yao, C., *Sep. Purif. Technol.*, 2000, vol. 19, p. 237.
13. Sazama, P., Tvaruzkova, Z., Jirglova, H., and Sobalik, Z., *Stud. Surf. Sci. Catal.*, 2008, vol. 174, p. 821.
14. Al-Abadleh, H.A. and Grassian, V.H., *Langmuir*, 2003, vol. 19, p. 341.
15. Krylov, O.V., *Geterogennyi kataliz: Uchebnoe posobie* (Heterogeneous Catalysis: A Textbook), Novosibirsk: Novosibirsk. Gos. Univ., 2002, vol. 2.
16. Zotov, R.A., Molchanov, V.V., Goidin, V.V., Moroz, E.M., and Volodin, A.M., *Kinet. Catal.*, 2010, vol. 51, no. 1, p. 139.
17. Volodin, A.M., Bolshov, V.A., and Konovalova, T.A., *Mol. Eng.*, 1994, vol. 4, p. 201.
18. Bedilo, A.F. and Volodin, A.M., *Kinet. Catal.*, 2009, vol. 50, no. 2, p. 3314.
19. Bedilo, A.F., Ivanova, A.S., Pahomov, N.A., and Volodin, A.M., *J. Mol. Catal. A: Chem.*, 2000, vol. 158, no. 1, p. 409.
20. Buyanov, R.A., Krivoruchko, O.P., and Zolotovskii, B.P., *Izv. Sib. Otd. Akad. Nauk SSSR, Ser. Khim. Nauki*, 1986, vol.4, no. 11, p. 39.
21. Dzis'ko, V.A. and Ivanova, A.S., *Izv. Sib. Otd. Akad. Nauk SSSR*, 1985, vol. 5, no. 15, p. 110.
22. Shefer, K.I., *Cand. Sci. (Chem.) Dissertation*, Novosibirsk: Inst. of Catalysis, 2008.
23. Gregg, S.J. and Sing, K.S.W., *Adsorption, Surface Area and Porosity*, New York: Academic, 1982.
24. Fenelonov, V.B., *Vvedenie v fizicheskuyu khimiyu formirovaniya supramolekulyarnoi struktury adsorbentov i katalizatorov* (Introduction to the Physical Chemistry of the Formation of the Supramolecular Structure of Adsorbents and Catalysts), Novosibirsk: Sib. Otd. Ross. Akad. Nauk, 2004.
25. Malyshev, M.E., Paukshtis, E.A., Malysheva, L.V., Toktarev, A.V., and Vostrikova, L.A., *Kinet. Catal.*, 2005, vol. 46, no. 1, p. 100.
26. Paukshtis, E.A., *Infrakrasnaya spektroskopiya v geterogennom kislotno-osnovnom katalize* (Infrared Spectroscopy Applied to Heterogeneous Acid–Base Catalysis), Novosibirsk: Nauka, 1992.
27. Zotov, R.A., Molchanov, V.V., Volodin, A.M., and Bedilo, A.F., *J. Catal.*, 2011, vol. 278, p. 71.